

Heterogeneous & Homogeneous & Bio- & Nano-

CHEM **CAT** CHEM

CATALYSIS

Accepted Article

Title: Insight into the correlation between Cu species evolution and ethanol selectivity in the direct ethanol synthesis from CO hydrogenation

Authors: Xiaoli Li, Guohui Yang, Meng Zhang, Xiaofeng Gao, Hongjuan Xie, Yunxing Bai, Yingquan Wu, Junxuan Pan, and Yisheng Tan

This manuscript has been accepted after peer review and appears as an Accepted Article online prior to editing, proofing, and formal publication of the final Version of Record (VoR). This work is currently citable by using the Digital Object Identifier (DOI) given below. The VoR will be published online in Early View as soon as possible and may be different to this Accepted Article as a result of editing. Readers should obtain the VoR from the journal website shown below when it is published to ensure accuracy of information. The authors are responsible for the content of this Accepted Article.

To be cited as: *ChemCatChem* 10.1002/cctc.201801888

Link to VoR: <http://dx.doi.org/10.1002/cctc.201801888>

Insight into the correlation between Cu species evolution and ethanol selectivity in the direct ethanol synthesis from CO hydrogenation

Xiao-Li Li,^[a,b] Guo-Hui Yang,^[a] Meng Zhang,^[a,b] Xiao-Feng Gao,^[a,b] Hong-Juan Xie,^[a]
Yun-Xing Bai,^[a, b] Ying-Quan Wu,^[a] Jun-Xuan Pan,^[a] and Yi-Sheng Tan^{[a,c]*}

Cu/SiO₂ catalyst was prepared by the ammonia evaporation method for the direct synthesis of ethanol from CO hydrogenation. The catalyst exhibited the initial ethanol selectivity as high as 40.0 wt%, which dramatically decreased from 40.0 to 9.6 wt% on the stream of 50 h. XRD, XPS, TEM and N₂O titration techniques were employed to elucidate the ethanol selectivity change and catalyst structure evolution during reaction process. The experiment and characterization results indicated that both Cu⁺/(Cu⁺+Cu⁰) value and copper crystallite size had great effects on the ethanol selectivity. During the initial 38 h, the ethanol selectivity obviously decreased from 40.0 to 18.2 wt%, and Cu⁺/(Cu⁺+Cu⁰) value on the catalyst surface rapidly dropped from 0.67 to 0.39, while the copper crystallite size remained almost unchanged. However, during the reaction period of 38-50 h, the Cu⁺/(Cu⁺+Cu⁰) value possessed no distinct change, but a further decrease in ethanol selectivity and a rapid aggregation in Cu particles were observed simultaneously. The present systematic investigation demonstrated that the decrease of Cu⁺/(Cu⁺+Cu⁰) value was the main factor for the loss of ethanol selectivity during the initial 38 h, whereas the rapid growth of Cu particles during the reaction period of 38-50 h were mainly contributed to the further decline of ethanol selectivity.

Introduction

Ethanol is widely used as fuel, fuel additive, and even a potential substitute for gasoline [1-2]. Besides, it is also an important intermediate for value-added fine chemicals [3-4]. With increasing concerns for environmental pollution and depletion of nonrenewable petroleum resources, the direct synthesis of ethanol from CO hydrogenation, since its high atom economy and low waste emission, has attracted growing attention in a few decades [4-6].

Typically, suitable catalysts for higher alcohols synthesis from CO hydrogenation can be divided into the following types: the modified Cu-based methanol synthesis catalysts [7, 8], the modified Fischer-Tropsch synthesis catalysts [9], the Mo-based catalysts [10-12] and the Rh-based catalysts [13]. Among these catalysts, the Cu-based catalysts have been widely investigated because of their high activity and low price [3, 14-17]. It was found that the ethanol selectivity could achieve ~ 40 Cmol% in the direct ethanol synthesis from CO hydrogenation over Cu-based catalysts [7, 9-11, 14-17]. Unfortunately, the previous Cu-based catalysts employed for direct synthesis ethanol from CO hydrogenation generally suffered a rapid deactivation, especially the decline in ethanol selectivity, which limited its further large-scale application.

It is generally thought that Cu dispersion and/or the distribution of Cu⁰ and Cu⁺ species have great influence on the product selectivity during the hydrogenation process over Cu-based catalysts [18-26]. Tuning catalyst preparation parameters (e.g. promoters [18-22], Cu loading [23-26], calcination temperature [24]) of Cu-based catalysts is really efficient to modify Cu dispersion and Cu⁺/(Cu⁰ + Cu⁺) value. According to the previous literatures, it is plausible that both more dispersed Cu species and higher Cu⁺/(Cu⁰+Cu⁺) value are effective to improve the product selectivity. However, since the catalyst preparation process is tedious, the above-mentioned catalyst system is too complicated to obtain a clear and intrinsic explanation on the evolution of catalyst structure during the reaction process.

To rule out the influence of catalyst preparation parameters on catalyst structure, comparing the catalyst structure at the reduced and spent stages is an alternative approach to clarify the structure-performance relationship of Cu-based catalysts for hydrogenation process. Sun et al. [27] pointed out that the severe sintering and the formation of CoxC species on the used catalyst caused the decline of activity. Sahibzada et al. [28] studied the loss of Cu/ZnO/Al₂O₃ activity for methanol synthesis from CO hydrogenation. They demonstrated a similar conclusion that the decrease in methanol selectivity was resulted from the

^a State Key Laboratory of Coal Conversion, Institute of Coal Chemistry, Chinese Academy of Sciences, Taiyuan 030001, China

^b University of Chinese Academy of Sciences, Beijing 100049, China

^c National Engineering Research Center for Coal-Based Synthesis, Institute of Coal Chemistry, Chinese Academy of Sciences, Taiyuan 030001, China

E-mail addresses: tan@sxicc.ac.cn; Tel. / fax: +086-351-4044287

sintering of Cu particles. Shen et al. [29] found that the Cu/SiO₂ catalyst showed outstanding activity with a total selectivity of 95 % for ethanol and methanol during dimethyl oxalate (DMO) hydrogenation. It was found that the average size of copper particles kept unchanged in the spent catalyst, but the Cu⁺/(Cu⁰+Cu⁺) ratio increased during the course of reaction. By comparing the reduced and used catalysts, Zhao et al. [30] reported that the activity loss of ethanol formation from DMO over Cu/SiO₂ catalysts was mainly attributed to the destruction of suitable surface Cu⁺ and Cu⁰ distribution and to the decline of Cu dispersion. T. Williams et al. [31] also found that the imbalance of Cu⁺ and Cu⁰ species and crystallite aggregation resulted in rapid decrease of ethanol selectivity during DMO hydrogenation. Comparing the structure changes on the reduced and spent catalysts provided a superficial understanding of the relation between structure evolution and performance of Cu-based catalysts. However, the main factor, which influenced the performance (activity and/or selectivity) change, was still equivocal and controversial.

Based on the above literatures, we are convinced that investigating the correlation between Cu species evolution and performance over a simplified catalytic system is vital to explore the key factor on ethanol selectivity change during the reaction process. In heterogeneous catalysis, metals or metal oxides are traditionally dispersed as nanoscale particles on a support with a large surface to maximize the number of exposed active sites [32]. As reported [33-36], copper species are much easier to be highly dispersed on Al₂O₃ or SiO₂ support with large surface in comparison to the TiO₂ support with a small surface. Despite that Al₂O₃ support has been used for widespread applications, the relatively high quantity of acid sites on Al₂O₃ surface may catalyze unwanted isomerization or oligomerization reactions according to many studies [28, 32, 36, 38]. Therefore, in the present study, an inert SiO₂ support with a large surface was considered as a suitable choice [20-23, 39].

In this work, we prepared a simple Cu/SiO₂ catalyst using the ammonia evaporation method and evaluated its performance for ethanol synthesis from CO hydrogenation. The ethanol selectivity at initial 14.5 h over the catalyst achieved to 40.0 wt% but sharply decreased to 9.6 wt% when the reaction time was enhanced to 50 h. In the whole reaction process, the major alcohol products were methanol and ethanol (above 98.9 wt%). To elucidate the reason for the decline of ethanol selectivity, the evolution of Cu/SiO₂ catalyst structure at different stages was

investigated by the characterization techniques, including X-ray diffraction (XRD), X-ray photoelectron spectroscopy (XPS), Transmission electron microscope (TEM) and N₂O titration. Furthermore, the correlation between the structure evolution and the decrease of ethanol selectivity during reaction process was systematically discussed.

Results and Discussion

Performance of Cu/SiO₂ catalyst

The performance of Cu/SiO₂ catalyst for ethanol synthesis via CO hydrogenation was evaluated and the results were presented in Fig. 1. The total alcohols selectivity showed a decrease trend (from 30.2 to 23.9 %) with reaction time. Obviously, the primary products over Cu/SiO₂ catalyst were methanol and ethanol (~98.9 wt%) during the whole reaction process, while the selectivity of ethanol sharply decreased from 40.0 to 9.6 wt%, simultaneously, methanol selectivity dramatically increased from 58.9 to 90.0 wt%. Here, in order to investigate the relation between the structure evolution and loss of ethanol selectivity during reaction, the Cu/SiO₂ catalyst at different stages was studied by XRD, XPS, TEM and N₂O titration.

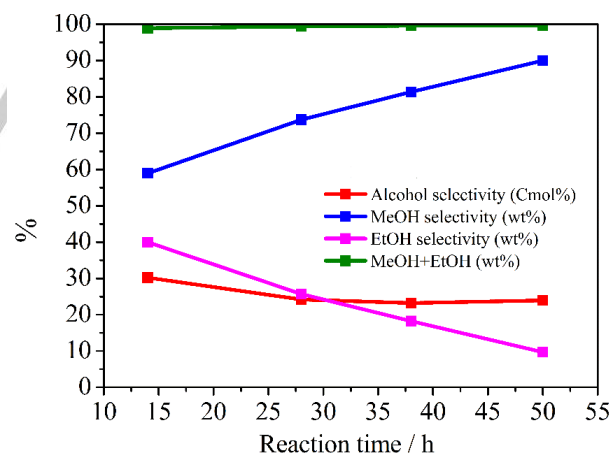


Fig. 1. Performance of Cu/SiO₂ catalyst for CO hydrogenation as a function of reaction time
Reaction conditions: T = 300 °C, P = 3 MPa, GHSV = 5000 h⁻¹, H₂/CO = 2.5.

Catalyst characterization

Fig. 2 showed the XRD patterns of CS-calcined, CS-reduced, CS-reaction-14.5 h, CS-reaction-28 h, CS-reaction-38 h and CS-reaction-50 h, in which the diffraction peak at around 22° came from amorphous silica [34]. The XRD pattern of the CS-calcined sample showed two strong diffraction peaks at 2θ of

35.6 and 38.7° along with two weak peaks at 48.8 and 61.5°, which were attributed to the typical peaks of CuO (JCPDS no. **05-0661**) [40-42]. For CS-reduced sample, the peaks of CuO phase almost disappeared, accompanied by the observable Cu₂O peaks at 36.6 and 42.4° (JCPDS no. **034-1354**). It indicated that most of CuO phase could be reduced to Cu⁺ species after reduced in the fixed-bed reactor, consistent with the previous report by Zhao et al. [30]. It was found that the peaks of Cu₂O were dramatically weakened with the enhancement of reaction time until they were vanished when the reaction was evaluated to 50 h. Meanwhile, three weak diffraction peaks at 2θ of 43.3°, 50.4° and 74.1° for Cu (JCPDS no. **04-0836**) emerged in CS-reaction-14.5 h sample [19]. The intensities of Cu diffraction peaks remained almost unchanged in the first 38 h but displayed an obvious growing with a further increase of reaction time. The significant sharpening of Cu diffraction peaks indicated that Cu particles possessed a severe aggregation during the reaction process, which is probably because that the reaction temperature (300 °C) in this work is higher than the Hüttig temperature of Cu (134 °C) [43] and the CO hydrogenation to ethanol is an exothermic reaction. From the calculation results based on the Scherrer equation (**Table 1**), the Cu crystallite size showed a quite slight growth before 38 h and markedly increased from 15.8 to 27.3 nm when the reaction time increased from 38 to 50 h. These results clearly revealed that the CuO phase could transform into Cu₂O during the reduction process and the Cu₂O species would be further gradually reduced into metallic Cu during the CO hydrogenation process [26, 30].

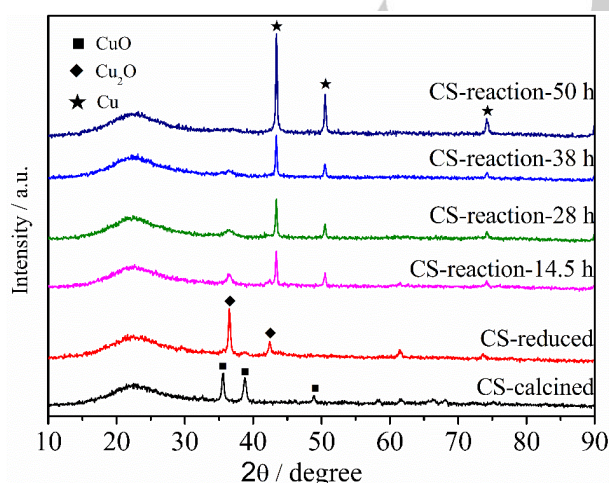


Fig. 2. XRD patterns of catalysts: CS-calcined, CS-reduced, CS-reaction-14.5 h, CS-reaction-28 h, CS-reaction-38 h and CS-reaction-50 h

Table 1 Crystallite sizes of CuO, Cu₂O and Cu over CS-calcined, CS-reduced, CS-reaction-14.5 h, CS-reaction-28 h, CS-reaction-38 h and CS-reaction-50 h catalysts

Samples	Crystallite sizes (nm) ^[a]		
	CuO	Cu ₂ O	Cu
CS-calcined	14.4	-	-
CS-reduced	5.0	18.1	-
CS-reaction-14.5 h	-	9.7	13.7
CS-reaction-28 h	-	6.5	14.9
CS-reaction-38 h	-	5.9	15.8
CS-reaction-50 h	-	-	27.3

[a] CuO, Cu₂O and Cu crystallite sizes calculated by the Scherrer formula

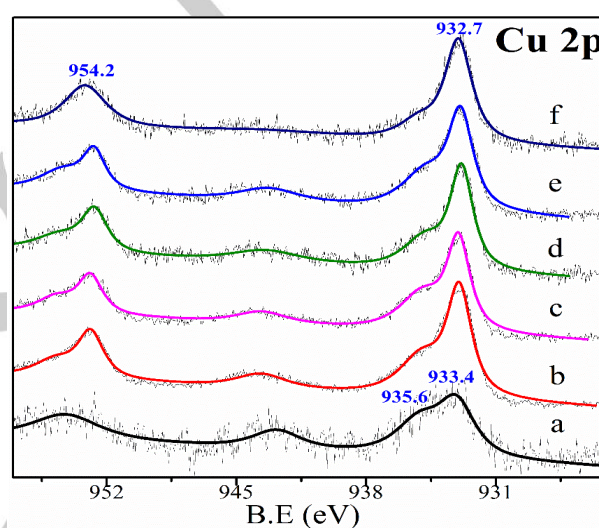


Fig. 3. Cu 2p XPS spectra of catalysts: (a) CS-calcined (b) CS-reduced (c) CS-reaction-14.5 h (d) CS-reaction-28 h (e) CS-reaction-38 h (f) CS-reaction-50 h

XPS analysis was carried out to elucidate the chemical states of Cu species. As displayed in **Fig. 3**, for the CS-calcined sample, the Cu 2p_{3/2} peak at ~933.0 eV, Cu 2p_{1/2} peak at ~954 eV and the satellite peak at 942-944 eV could be observed, indicating that copper existed in the oxidation state of +2 [44]. Considering the asymmetry of the Cu 2p_{3/2} envelope, the peak of CS-calcined sample could be deconvoluted into two contributions centered around 933.4 and 935.6 eV, which were corresponding to CuO and copper phyllosilicate, respectively [42]. After the sample was reduced, the peak at 933.4 eV of CuO shifted toward lower BEs (932.7eV), revealing that the CuO phase was reduced to a low valence state of +1 or 0. However, the peak at 935.6 eV of copper phyllosilicate and the satellite peak at 942-944 eV were still detectable in the CS-reduced sample, confirming that a temperature of 300 °C was insufficient

to reduce the CS-calcined sample due to the strong interaction between silica support and Cu species. It was found that the characteristic peaks of copper phyllosilicate (935.6 eV) and Cu 2p satellite peak (942-944 eV) apparently weakened along with the reaction time and disappeared at 50 h. It suggested that most of Cu^{2+} species were reduced to Cu^+ or Cu^0 when reaction time was 50 h. These results revealed that the copper valence transition occurred during CO hydrogenation.

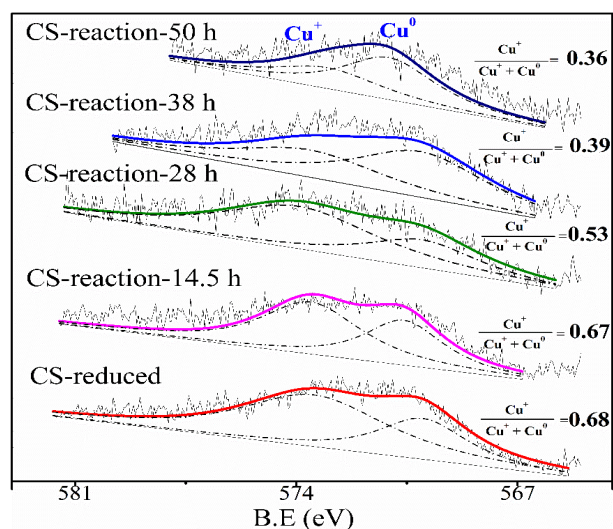


Fig. 4. XAES spectra of catalysts: CS-calcined, CS-reduced, CS-reaction-14.5 h, CS-reaction-28 h, CS-reaction-38 h and CS-reaction-50 h

The amount of Cu^+ and Cu^0 could be determined via X-ray auger electron spectra (XAES). In the XAES spectra of CS-reduced sample (**Fig. 4**), the appearance of two obvious overlapping peaks at around 570 and 574 eV was employed to distinguish between Cu^0 and Cu^+ species [23, 45]. From the deconvolution results (**Fig. 4**), the molar ratio of the surface $\text{Cu}^+ / (\text{Cu}^0 + \text{Cu}^+)$ was significantly affected by reaction time. The

$\text{Cu}^+ / (\text{Cu}^+ + \text{Cu}^0)$ value dramatically decreased from 0.67 to 0.39 within first 38 h and tended to be stable after 38 h. These results indicated that the chemical states of copper species in Cu/SiO_2 catalyst underwent changes during reaction, which directly affected the $\text{Cu}^+ / (\text{Cu}^+ + \text{Cu}^0)$ value.

The TEM images of CS-calcined, CS-reduced, CS-reaction-14.5 h, CS-reaction-28 h, CS-reaction-38 h and CS-reaction-50 h were given in **Fig. 5**. It was easily observed that the metal nanoparticles were distributed uniformly on the silica surface for the catalyst after calcined. As shown in **Fig. 5**, the particle diameter distribution possessed the mean particle size of approximately 5.2 nm on the CS-reduced sample. In addition, the average crystallite size did not obviously increase (5.0 ~ 5.8 nm) before 38 h, while the particle size grew significantly from 5.8 to 8.9 nm when the reaction time increased from 38 to 50 h. These results were in good agreement with XRD.

The Cu^0 surface areas ($S_{\text{Cu}(0)}$) of CS-reaction-14.5 h (187.4 $\text{m}^2/\text{g-Cu}$), CS-reaction-28 h (193.1 $\text{m}^2/\text{g-Cu}$), CS-reaction-38 h (186.9 $\text{m}^2/\text{g-Cu}$) and CS-reaction-50 h (116.0 $\text{m}^2/\text{g-Cu}$) catalysts were measured using N_2O titration. During the initial 38 h, the $S_{\text{Cu}(0)}$ value ($\sim 190 \text{ m}^2/\text{g-Cu}$) remained almost unchanged. Interestingly, Cu particle size did not obviously change before 38 h, as revealed by XRD and TEM results. Nevertheless, the $S_{\text{Cu}(0)}$ value clearly decreased from 186.9 to 116.0 $\text{m}^2/\text{g-Cu}$ when the reaction time increased from 38 to 50 h, resulted from the aggregation of Cu particles [3, 20, 26, 30, 43]. Consistently, the above-discussed XRD and TEM results showed the similar variation trend during the reaction period of 38-50 h. Thus, the evolution of Cu particle size was systematically investigated based on the aforementioned characterizations including XRD, TEM and N_2O titration.

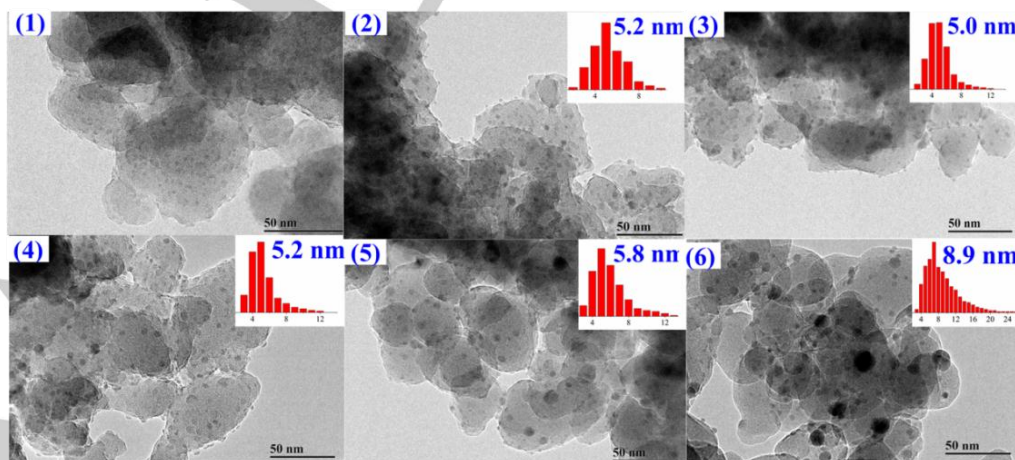


Fig. 5. TEM images of catalysts: (1) CS-calcined, (2) CS-reduced, (3) CS-reaction-14.5 h, (4) CS-reaction-28 h, (5) CS-reaction-38 h and (6) CS-reaction-50 h

Discussion of Cu species evolution

Fig. S1 showed the in situ XRD patterns of Cu/SiO₂ catalyst during the reduction and reaction process. In accordance with the results displayed in **Fig. 2**, the XRD pattern of the CS-calcined sample showed three strong diffraction peaks at 2θ of 35.6, 38.7 and 48.8°, ascribed to the typical peaks of CuO (JCPDS no. **05-0661**) [40-42]. During the reduction process, it is easily observed that the intensities of CuO diffraction peaks decreased gradually, accompanied by the observable Cu₂O peaks at 36.5 and 42.4° (JCPDS no. **034-1354**). Moreover, after reduction treatment, most of CuO phase could be reduced to Cu⁺ species. When the catalyst was exposed under the H₂/CO mixture gas, the peaks of Cu₂O were dramatically weakened with the enhancement of operation time. Simultaneously, three diffraction peaks at 2θ of 43.3°, 50.4° and 74.0° for Cu (JCPDS no. **04-0836**) emerged [19]. The intensities of Cu diffraction peaks increased slightly in the initial reaction period but displayed an obvious growth with time further increased, which indicated that Cu particles possessed a severe aggregation. These results were in good agreement with the discussion of the conventional XRD.

According to the XRD (including conventional and in situ results) and XPS analysis, it was suggested that the Cu₂O species can be reduced into metallic Cu, thereby resulting in the decrease of Cu⁺/(Cu⁺+Cu⁰) value with reaction time. H. Oguchi and his co-workers [46, 47] reported that Cu₂O was more stable than Cu metal. It revealed that, when the Cu⁺/(Cu⁺+Cu⁰) value was high, the high Cu⁺ species density around Cu⁰ species could efficiently fix copper species and retard the particle growth. However, when Cu⁺/(Cu⁺+Cu⁰) value was below a certain value, the metallic Cu migration was not able to be suppressed because of the relatively low Cu⁺ species density. Thus, the rapid aggregation of Cu particles occurred inevitably during the reaction period of 38-50 h (XRD, TEM, N₂O titration).

Based on the characterizations above, the proposed Cu species evolution over Cu/SiO₂ catalyst was displayed in **Fig. 6**. As described in **Fig. 6**, the copper species were highly dispersed on the silica surface. Cu₂O phase (Cu⁺ species) was the main copper species and high Cu⁺/(Cu⁺+Cu⁰) value was detected in the CS-reduced sample. After reduced, feed gas (CO + H₂) was introduced into the reactor. Cu₂O (Cu⁺ species) gradually reduced into metallic Cu with reaction time and thus the value of

Cu⁺/(Cu⁺+Cu⁰) declined. When the Cu⁺/(Cu⁺+Cu⁰) value was relatively high, the high Cu⁺ species density around Cu⁰ species could efficiently fix copper species and, hence, the particle size remained unchanged. However, when Cu⁺/(Cu⁺+Cu⁰) value was below a certain value, due to the lower Hütting temperature of Cu (134 °C) [44, 46, 47] and the exothermic CO hydrogenation, the low amount of Cu⁺ species in vicinity of metallic Cu could not hamper the metallic Cu of migrating, consequently resulting in the migration and aggregation of Cu particles.



Fig. 6. Schematic representation of the deactivation of Cu/SiO₂ catalyst

Study on the correlation between structural evolution and the change of ethanol selectivity

In the entire process of CO hydrogenation, the primary products over Cu/SiO₂ catalyst were methanol and ethanol (above 98.9%). During reaction, the selectivity of ethanol sharply decreased from 40.0 to 9.6 wt%, while methanol selectivity dramatically increased from 58.9 to 90.0 wt%. According to the characterization results, the CuO phase was observed in CS-calcined sample, and most of CuO phase (Cu⁺ species) transformed into Cu₂O after reduction treatment and then the Cu⁺ species could be further reduced to Cu⁰ species gradually with reaction time (**Fig. 2, 3**). The Cu⁺/(Cu⁺+Cu⁰) value on the catalyst surface significantly dropped from 0.67 to 0.39 during the initial 38 h and tended to be stable after 38 h (**Fig. 4**). Conversely, the copper crystallite size did not change obviously before 38 h, but it grew rapidly with the further increase of reaction time (**Fig. 2, 5**). Here, a plot of ethanol selectivity, Cu⁺/(Cu⁺+Cu⁰) value and copper crystallite size versus reaction time was presented in **Fig. 7**. It was obvious that both the Cu⁺/(Cu⁺+Cu⁰) value and copper crystallite size influenced the ethanol selectivity. To further understand the correlation between

Cu species evolution and ethanol selectivity change during the reaction, **Fig. 7** can be roughly divided into two stages: 0-38 and 38-50 h.

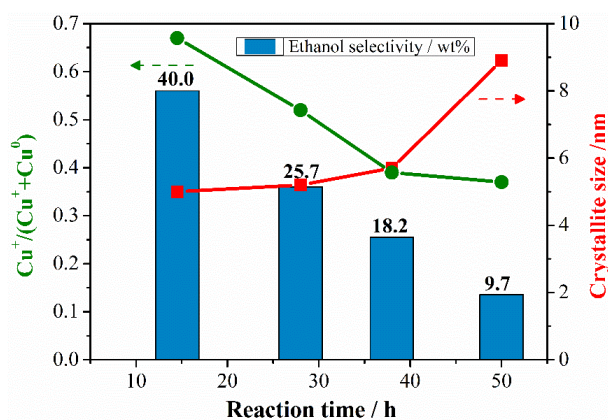


Fig. 7. Ethanol selectivity, $\text{Cu}^+ / (\text{Cu}^+ + \text{Cu}^0)$ and Crystallite size as a function of reaction time

During the initial 38 h, the ethanol selectivity decreased from 40.0 to 18.2 wt%. The value of $\text{Cu}^+ / (\text{Cu}^+ + \text{Cu}^0)$ declined sharply, while the copper crystallite size kept almost unchanged. This result revealed that the $\text{Cu}^+ / (\text{Cu}^+ + \text{Cu}^0)$ value was closely related to ethanol formation before 38 h. Ma et al. reported [23, 30, 44] that the Cu^0 species boosted the H_2 decomposition and Cu^+ species facilitated the C-O cleavage in CH_xO by polarizing the C=O bond to increase the content of CH_x species, thus favoring the formation of ethanol. The authors also pointed out that the synergy effect of $\text{Cu}^+ - \text{Cu}^0$ species required a suitable amount of the two sites in catalyzing methyl acetate to ethanol. In addition, in our previous studies on K-Cu/ Al_2O_3 catalysts [37], we found that the synergy of Cu^+ and Cu^0 species played an important role in ethanol synthesis via CO hydrogenation. Hence, the cooperation of Cu^+ and Cu^0 sites on the catalyst surface should be considered as a key cause for the loss of ethanol selectivity during the initial 38 h. A possible mechanism of ethanol synthesis from CO hydrogenation was proposed in this work (**Fig. 8**). As displayed in **Fig. 8**, the Cu^0 species on the Cu/ SiO_2 catalyst surface boosted the H_2 decomposition and provided H species [13, 23, 44, 48]. The CH_xO species, formed by CO hydrogenation, has been considered as the key reactive intermediates involved in ethanol formation [49] and Cu^+ species as electrophilic or Lewis acidic sites were proposed to act toward accelerating the C-O cleavage in CH_xO to give CH_x species [13, 23]. Then, the CH_xCO species formed by CO insertion into CH_x and terminated by H species, thereby turning

into ethanol (The results of in situ Fourier transform infrared convinced our assumption and the relevant results and discussion were put in supporting information.). When $\text{Cu}^+ / (\text{Cu}^+ + \text{Cu}^0)$ value decreased, as shown in **Fig. 8**, the decrease in the amounts of Cu^+ sites restrained the C-O cleavage in CH_xO , and the amounts of CH_x species was bound to decline, which inevitably resulted in a decrease in ethanol selectivity. Meanwhile, the content of CH_xO species increased on the catalyst surface by limiting the C-O cleavage in CH_xO . Then, the CH_xO species basically underwent a step-wise hydrogenation to methanol. Thus, methanol selectivity significantly improved with decreasing in the $\text{Cu}^+ / (\text{Cu}^+ + \text{Cu}^0)$ value (**Fig. 1**).

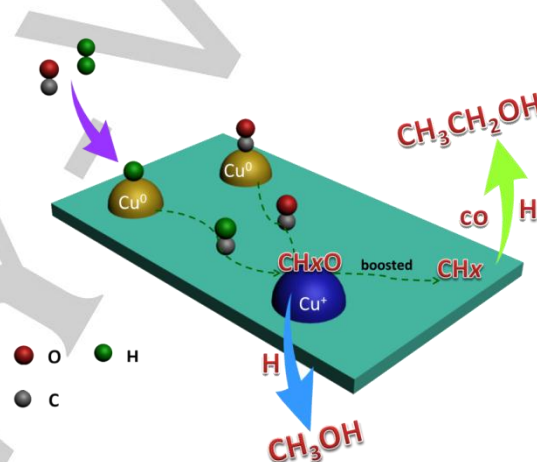


Fig. 8. Schematic representation of methanol and ethanol from CO hydrogenation over Cu/ SiO_2 catalyst

During the reaction period of 38-50 h, the ethanol selectivity still showed a continuing decrease, although the $\text{Cu}^+ / (\text{Cu}^+ + \text{Cu}^0)$ value did not change significantly, the value of $\text{Cu}^+ / (\text{Cu}^+ + \text{Cu}^0)$ after 38 h were so small that the low Cu^+ species density in vicinity of metallic Cu could not hamper the migration of Cu particles (Cu_2O was more stable than Cu metal [46, 47]). Moreover, the exothermic CO hydrogenation also boosted the accumulation of Cu particles. Thus, the further decrease in ethanol selectivity may be caused by the aggregation of Cu particles when the reaction time increased from 38 to 50 h (**Fig. 7**). In addition, a further increase in selectivity of methanol was also observed during the reaction period of 38-50 h (**Fig. 1**). Arena et al. [50] used Cu/Zn/Zr catalysts with Cu particle size from 2 to 25 nm for methanol synthesis and found that selectivity to methanol was favored over catalysts possessing larger copper nanoparticles. It suggested that larger Cu particles after

38 h promoted methanol formation in our present experiment.

In the entire process of CO hydrogenation, it should be noted that despite a continuous decrease in ethanol selectivity, the main factor which led to the result was different during the different stages. Specifically, highly dispersed CuO species on the calcined catalyst were reduced into Cu₂O phase (Cu⁺ species) after reduction treatment, accompanied by a high Cu⁺/(Cu⁺+Cu⁰) value, which was a crucial factor in ethanol formation from CO hydrogenation. After reduced, when the catalyst was exposed under the H₂/CO mixture gas, Cu₂O (Cu⁺ species) gradually transformed into metallic Cu with increased time. Apparently, both the Cu⁺/(Cu⁺+Cu⁰) value and ethanol selectivity declined, however, the Cu particle size occupied a stable state. When Cu⁺/(Cu⁺+Cu⁰) value decreased to a certain value, the low amount of Cu⁺ species in vicinity of metallic Cu could not hamper the metallic Cu migration and thus resulted in the aggregation of Cu particles, which inevitably further led to the loss of ethanol selectivity.

Conclusions

Studying the relation between Cu species evolution and ethanol selectivity over Cu/SiO₂ catalyst for ethanol synthesis from CO hydrogenation would provide a theoretical basis for designing an efficient catalyst in terms of improving ethanol selectivity and stability. In the present work, a simplified catalytic system Cu/SiO₂ catalyst prepared by the ammonia evaporation method was studied for ethanol synthesis from CO hydrogenation and the correlation of catalyst structure evolution and ethanol selectivity change was investigated. The Cu/SiO₂ catalyst exhibited a high initial ethanol selectivity of 40.0 wt%. But it dramatically decreased to 9.6 wt% when the reaction time was enhanced to 50 h. According to the characterization results (at different stages), both copper valence and copper crystallite size underwent changes during the CO hydrogenation process. During the initial 38 h, the Cu⁺/(Cu⁺+Cu⁰) value on the surface of Cu/SiO₂ catalyst rapidly dropped from 0.67 to 0.39, while the copper crystallite size remained almost unchanged. During the reaction period of 38-50 h, the Cu⁺/(Cu⁺+Cu⁰) value did not change significantly, but Cu⁺/(Cu⁺+Cu⁰) value was so small that could not hamper the Cu particles migration, thus resulting in an inevitable occurrence of the Cu particles accumulation. Combined with the experimental results, both the Cu⁺/(Cu⁺+Cu⁰)

value and copper crystallite size were considered to be contributed to ethanol formation from CO hydrogenation within 50 h. In the beginning 38 h, the decrease in Cu⁺/(Cu⁺+Cu⁰) value led to the loss of ethanol selectivity. During the reaction from 38 to 50 h, the rapid growth of Cu particle further decreased in ethanol selectivity. Thus, designing a catalyst possessing relatively small Cu particles and high Cu⁺/(Cu⁺+Cu⁰) value may be a promising prospect to improving ethanol selectivity and stability from CO hydrogenation over Cu-based catalysts.

Experimental Section

Materials

The analytical-grade chemical Cu(NO₃)₂·3H₂O (99%) was purchased from the Beijing Chemical Co., Ltd., and used directly without further purification. The employed SiO₂ was purchased from Aladdin Industrial Co.

The preparation of Cu/SiO₂ catalyst

The Cu/SiO₂ catalyst was prepared using the ammonia evaporation method, briefly described as follows. 5.33 g of Cu(NO₃)₂·3H₂O was dissolved in 100.00 mL of ethanol. Then, 100.00 mL of 28 % ammonia aqueous solution was added and stirred for 20 min. Subsequently, 10.00 g SiO₂ was added into the copper ammonia complex solution, stirred in ultrasonic wave for 1 h at room temperature. After that, the suspension was transferred into a Teflon-lined stainless autoclave and heated at 180 °C for 6 h. The obtained precipitate was collected, filtered, washed with ethanol and deionized water carefully. Finally, the mixture was dried at 120 °C for 10 h and the dried precursor was calcined under static air at 450 °C for 5 h. The resulted Cu/SiO₂ catalyst was tableted, crushed, sieved to 30-40 mesh, and denoted as CS-calcined, where C and S indicated CuO, and SiO₂, respectively. The reduced catalyst was denoted as CS-reduced and the used catalysts were simplified as CS-reaction-*t* (*t* = 14.5, 28, 37 and 50 h), where “*t*” represented the reaction time.

Catalyst characterization

The structure of CS-calcined, CS-reduced, CS-reaction-14.5 h, CS-reaction-28 h, CS-reaction-38 h and CS-reaction-50 h catalysts was studied by XRD, XPS, TEM and N₂O titration techniques. Before characterization, in order to keep the

structure of CS-reduced, CS-reaction-14.5 h, CS-reaction-28 h, CS-reaction-38 h and CS-reaction-50 h catalysts unchanged as far as possible, after taken out from the fixed-bed reactor, those catalysts were immediately filled with N₂ and crushed in an inert glove box.

Powder X-ray diffraction patterns (XRD) were recorded over the 2θ range from 5 to 90 ° using a Rigaku MiniFlex II X-ray diffractometer, which was operated at 40 kV and 40 mA with Cu Kα radiation (λ = 0.15418 nm).

In situ XRD patterns of the catalyst were recorded over the 2θ range from 30 to 80 ° equipped with an XRD900 instrument, which was operated at 40 kV and 40 mA with Cu Kα radiation (λ = 0.15418 nm). The CS-calcined catalyst was heated to 300 °C at a rate of 10 °C/min under a flow of 10 % H₂/N₂ mixture gas, kept at that temperature for 4 h. After reduction treatment, CO/H₂ (1/2.5) mixture gas was introduced into the flow system at 300 °C.

X-ray photoelectron spectroscopy (XPS) and X-ray auger electron spectroscopy (XAES) were used to analyze the change in the surface composition using an AXIS ULTRA DLD instrument equipped with Al Kα (hν = 1486.6 eV). Charging effects were corrected using the C 1s peak due to adventitious carbon with E_B fixed at 284.5 eV.

The information about the catalyst morphology was recorded using a field emission transmission electron microscope (HRTEM, JEM-2100 F), which was operated at 200 kV.

Copper surface area of the catalyst in different stages during reaction was determined by N₂O titration at 50 °C using the procedure described by H. Xi et al. [32] and Z. Yuan et al. [33]. In order to obtain the copper surface area (S_{Cu(0)}) under reaction temperature (300 °C), the used catalyst was pretreated by 5 % oxygen at 300 °C for 30 min and cooled to 30 °C, which totally oxidized the metallic Cu. After that, the catalyst was reduced by 10 % H₂/Ar (15 mL/min) with the temperature increasing from 30 to 300 °C and keeping for 1 h. The amount of consumed H₂ was measured and marked as X. And then, the catalyst was cooled down to 50 °C under Ar. The surface copper atoms were oxidized to Cu₂O in 5 % N₂O/Ar (15 mL/min) at 50 °C for 20 min. Finally, the catalyst was reduced by 10 % H₂/Ar (15 mL/min) with the temperature increasing to 300 °C at a rate of 10 °C/min. The amount of consumed H₂ in the second TPR was denoted as Y. The exposed Cu surface area at 300 °C was calculated by the following equation:

$$S_{Cu(0)} = \frac{2 \times Y \times N_{av}}{X \times M_{Cu} \times 1.4 \times 10^{19}} = \frac{1353 \times Y}{X} \text{ (m}^2\text{/g-Cu)}$$

where N_{av} = Avogadro's constant, M_{Cu} = relative atomic mass (63.456 g/mol), 1.4 × 10¹⁹ came from that an equal abundance of an average copper surface atom area of 0.0711 nm² (1.4 × 10¹⁹ copper atoms per square meter).

Here, S_{Cu(0)} represented the areas of surface Cu(0) at 300 °C (both the reduction temperature and reaction temperature were 300 °C).

Catalytic performance evaluation

The catalyst evaluation experiments were carried out in a stain-less fixed-bed reactor. The flow rate of feed gas was controlled by a mass flow controller, and the exit gas was measured by a wet flow meter. The reactions were conducted at a temperature of 300 °C and pressure of 3 MPa, using CO/H₂ = 1/2.5 at a space velocity of 5000 h⁻¹. Before reaction, the catalyst was reduced according to the designed temperature program, i.e. from room temperature to 300 °C, using a 10 % H₂/N₂ mixture for 4 h at 300 °C. The products during the reaction were analyzed using four GCs. The organic gas products, consisting of hydrocarbons and methanol, were detected online by flame ionization measurement using a GC4000A (GDX-403 column). The inorganic gas products were measured online by thermal conductivity measurement using a GC4000A (carbon molecular sieves column). The H₂O and methanol products in the liquid phase were detected by thermal conductivity measurement using a GC4000A (GDX-401 column). The alcohol products in the liquid phase were detected by flame ionization measurement using a GC-7AG (Chromosorb 101).

Acknowledgements

The authors are grateful for the financial support of National Natural Science Foundation of China (21573269) and the Key Research and Development Program of Shanxi Province.

Keywords: ethanol, CO hydrogenation, Cu-based catalyst, Cu⁺-Cu⁰ species, copper crystallite size.

References

- [1] L. X. Wang, L. Wang, J. Zhang, X. L. Liu, H. Wang, W. Zhang, Q. Yang, J. Y. Ma, X. Dong, S. J. Yoo, J. G. Kim, X. J. Meng, F. S. Xiao, *Angew. Chem. Int.*

- Ed.* **2018**, 130, 6212-6216.
- [2] Y. Wang, Y. J. Zhao, J. Lv, X. B. Ma, *ChemCatChem* **2017**, 9, 2085-2090.
- [3] H. R. Yue, X. B. Ma, J. L. Gong, *Acc. Chem. Res.* **2014**, 47, 1483-1492.
- [4] H. T. Luk, C. Mondelli, D. C. Ferre, J. A. Stewart, J. Pe'erez-Rami' rez, *Chem. Soc. Rev.* **2017**, 46, 1358-1426.
- [5] M. Devarapalli, H. K. Atiyeh, *Biofuel Res. J.* **2015**, 7, 268-280.
- [6] K. Göransson, U. Söderlind, J. He, W. Zhang, *Renewable Sustainable Energy Rev.* **2011**, 15, 482-492.
- [7] P. Wang, S. Y. Chen, Y. X. Bai, X. F. Gao, X. L. Li, K. Sun, H. J. Xie, G. H. Yang, Y. Z. Han, Y. S. Tan, *Fuel* **2017**, 195, 69-81.
- [8] L. Tan, G. H. Yang, Y. Yoneyama, Y. L. Kou, Y. S. Tan, T. Vitidsant, N. Tsubaki, *Appl. Catal. A.* **2015**, 505, 141-149.
- [9] Y. Z. Xiang, R. Barbosa, X. N. Li, N. Kruse, *ACS Catal.* **2015**, 5, 2929-2934.
- [10] S. F. Zaman, N. Pasupulety, A. A. Al-Zahrani, M. A. Daous, S. S. Al-Shahrani, H. Driss, L. A. Petrov, *Appl. Catal. A.* **2017**, 532, 133-145.
- [11] M. R. Morrill, N. T. Thao, H. Shou, R. J. Davis, D. G. Barton, D. Ferrari, P. K. Agrawal, C. W. Jones, *ACS Catal.* **2013**, 3, 1665-1675.
- [12] M. Konarova, F. Q. Tang, J. L. Chen, G. Wang, V. Rudolph, J. Beltramini, *ChemCatChem* **2014**, 6, 2394-2402.
- [13] Y. Choi, P. Liu, *J. Am. Chem. Soc.* **2009**, 131, 13054-13061.
- [14] M. Gupta, M. L. Smith, J. J. Spivey, *ACS Catal.* **2011**, 1, 641-656.
- [15] G. L. Liu, T. Niu, A. Cao, Y. X. Geng, Y. Zhang, Y. Liu, *Fuel* **2016**, 176, 1-10.
- [16] J. J. Su, Z. P. Zhang, D. L. Fu, D. Liu, X. C. Xu, B. F. Shi, X. Wang, R. Si, Z. Jiang, J. Xu, Y. F. Han, *J. Catal.* **2016**, 336, 94-106.
- [17] G. Prieto, S. Beijer, M. L. Smith, M. He, Y. Au, Z. Wang, D. A. Bruce, K. P. de Jong, J. J. Spivey, P. E. de Jongh, *Angew. Chem. Int. Ed.* **2014**, 53, 6397 – 6401.
- [18] Z. He, H. Q. Lin, P. He, Y. Z. Yuan, *J. Catal.* **2011**, 227, 54-63.
- [19] X. L. Zheng, H. Q. Lin, J. W. Zheng, X. P. Duan, Y. Z. Yuan, *ACS Catal.* **2013**, 3, 2738-2749.
- [20] Y. Wang, J. Y. Liao, J. Zhang, S. P. Wang, Y. J. Zhao, X. B. Ma, *AIChE J.* **2017**, 63 (7), 2839-2849.
- [21] P. P. Ai, M. H. Tan, N. Yamane, G. G. Liu, R. G. Fan, G. H. Yang, Y. Yoneyama, R. Q. Yang, N. Tsubaki, *Chem. Eur. J.* **2017**, 23, 8252-8261.
- [22] L. P. Han, L. Zhang, G. F. Zhao, Y. F. Chen, Q. F. Zhang, R. J. Chai, Y. Liu, Y. Lu, *ChemCatChem* **2016**, 8, 1065-1073.
- [23] Y. Wang, Y. Shen, Y. Zhao, J. Lv, S. Wang, X. Ma, *ACS Catal.* **2015**, 5, 6200-6208.
- [24] B. Wang, Y. Y. Cui, C. Wen, X. Chen, Y. Dong, W. L. Dai, *Appl. Catal. A.* **2016**, 509, 66-74.
- [25] T. Witoon, T. Numpilai, T. Phongamwong, W. Donphai, C. Boonyuen, C. Warakulwit, M. Chareonpanich, J. Limtrakul, *Chem. Eng. J.* **2018**, 334, 1781-1791.
- [26] R. P. Ye, L. Lin, J. X. Yang, M. L. Sun, F. Li, B. Li, Y. G. Yao, *J. Catal.* **2017**, 350, 122-132.
- [27] Y. Z. Yang, X. Z. Qi, X. X. Wang, D. Lv, F. Yu, L. S. Zhong, H. Wang, Y. H. Sun, *Catal. Today* **2016**, 270, 101-107.
- [28] J. T. Sun, I. S. Metcalfe, M. Sahibzada, *Ind. Eng. Chem. Res.* **1999**, 38, 3868-3872.
- [29] X. M. Huang, M. Ma, S. Miao, Y. P. Zheng, M. S. Chen, W. J. Shen, *Appl. Catal. A.* **2017**, 531, 79-88.
- [30] S. Zhao, H. R. Yue, Y. J. Zhao, B. Wang, Y. C. Geng, J. Lv, S. P. Wang, J. L. Gong, X. B. Ma, *J. Catal.* **2013**, 297, 142-150.
- [31] J. W. Zheng, J. F. Zhou, H. Q. Lin, X. P. Duan, C. T. Williams, Y. Z. Yuan, *J. Phys. Chem. C.* **2015**, 119, 13758-13766.
- [32] S. Soled, *Science* **2015**, 350(6265), 1171-1172.
- [33] J. J. Huang, T. Ding, K. Ma, J. M. Cai, Z. R. Sun, Y. Tian, Z. Jiang, J. Zhang, L. R. Zheng, X. G. Li, *ChemCatChem* **2018**, 10, 3862-3871.
- [34] D. X. Hu, H. L. Hu, H. Zhou, G. Z. Li, C. L. Chen, J. Zhang, Y. Yang, Y. P. Hu, Y. Y. Zhang, L. Wang, *Catal. Sci. Technol.* **2018**, 8, 6091-6099.
- [35] I. Obregón, I. Gandarias, A. Ocio, I. García-García, N. A. de Eulate, P. L. Arias, *Appl. Catal. B.* **2017**, 210, 328-341.
- [36] L. P. Han, L. Zhang, G. F. Zhao, Y. F. Chen, Q. F. Zhang, R. J. Chai, Y. Liu, Y. Lu, *ChemCatChem* **2016**, 8, 1065-1073.
- [37] X. L. Li, Q. D. Zhang, H. J. Xie, X. F. Gao, Y. Q. Wu, G. H. Yang, P. Wang, S. P. Tian, Y. S. Tan, *ChemistrySelect* **2017**, 2, 10365-10370.
- [38] P. Wang, S. Y. Chen, Y. X. Bai, X. F. Gao, X. L. Li, K. Sun, H. J. Xie, G. H. Yang, Y. Z. Han, Y. S. Tan, *Fuel* **2017**, 195, 69-81.
- [39] H. R. Yue, X. B. Ma, J. L. Gong, *Acc. Chem. Res.* **2014**, 47, 1483-1492.
- [40] H. J. Xi, X. N. Hou, Y. J. Liu, S. J. Qing, Z. X. Gao, *Angew. Chem. Int. Ed.* **2014**, 53, 11886-11889.
- [41] Z. L. Yuan, L. Wang, J. H. Wang, S. X. Xia, P. Chen, Z. Y. Hou, X. M. Zheng, *Appl. Catal. B.* **2011**, 101, 431-440.
- [42] Z. Q. Wang, Z. N. Xu, S. Y. Peng, M. J. Zhang, G. Lu, Q. S. Chen, Y. Chen, G. C. Guo, *ACS Catal.* **2015**, 5, 4255-4259.
- [43] H. R. Yue, Y. J. Zhao, L. Zhao, J. Lv, S. P. Wang, J. L. Gong, X. B. Ma, *AIChE J.* **2012**, 58, 2798-2809.
- [44] J. L. Gong, H. R. Yue, Y. J. Zhao, S. Zhao, L. Zhao, J. Lv, S. P. Wang, X. B. Ma, *J. Am. Chem. Soc.* **2012**, 134, 13922-13925.
- [45] Q. Wang, L. Qiu, D. Ding, Y. Z. Chen, C. W. Shi, P. Cui, Y. Wang, Q. H. Zhang, R. Liu, H. Shen, *Catal. Commun.* **2018**, 108, 68-72.
- [46] H. Oguchi, H. Kanai, K. Utani, Y. Matsumura, S. Imamura, *Appl. Catal. A.* **2005**, 293, 64-70.
- [47] H. Oguchi, T. Nishiguchi, T. Matsumoto, H. Kanai, K. Utani, Y. Matsumura, S. Imamura, *Appl. Catal. A.* **2005**, 281, 69-73.
- [48] X. F. Zhai, J. Shamoto, H. J. Xie, Y. S. Tan, Y. Z. Han, N. Tsubaki, *Fuel* **2018**, 87, 430-434.
- [49] Y. H. Zhao, K. J. Sun, X. F. Ma, J. X. Liu, D. P. Sun, H. Y. Su, W. X. Li, *Angew. Chem. Int. Ed.* **2011**, 50, 5335-5338.
- [50] F. Arena, K. Barbera, G. Italiano, G. Bonura, L. Spadaro, F. Frusteri, *J. Catal.* **2007**, 249, 185-194.

Entry for the Table of Contents

FULL PAPER

Both the $\text{Cu}^+ / (\text{Cu}^+ + \text{Cu}^0)$ values and copper crystallite sizes had great effects on the ethanol selectivity of Cu/SiO_2 catalyst



Xiao-Li Li, Guo-Hui Yang, Meng Zhang, Xiao-Feng Gao, Hong-Juan Xie, Yun-Xing Bai, Ying-Quan Wu, Jun-Xuan Pan, and Yi-Sheng Tan*

Page No. – Page No.

Insight into the correlation between Cu species evolution and ethanol selectivity in the direct ethanol synthesis from CO hydrogenation